

Spectral recovery of outdoor illumination by an extension of the Bayesian inverse approach to the Gaussian mixture model

Shahram Peyvandi,^{1,2,*} Seyed Hossein Amirshahi,¹ Javier Hernández-Andrés,³
Juan Luis Nieves,³ and Javier Romero³

¹Department of Textile Engineering, Amirkabir University of Technology, Tehran 15914, Iran

²Current address: Department of Psychology, Rutgers, The State University of New Jersey, Newark, New Jersey 07102, USA (e-mail: peyvandi@psychology.rutgers.edu)

³Departamento de Óptica, Facultad de Ciencias, Universidad de Granada, Granada 18071, Spain

*Corresponding author: peyvandi@aut.ac.ir

Received May 23, 2012; revised July 29, 2012; accepted August 13, 2012;
posted August 23, 2012 (Doc. ID 169212); published September 21, 2012

The Bayesian inference approach to the inverse problem of spectral signal recovery has been extended to mixtures of Gaussian probability distributions of a training dataset in order to increase the efficiency of estimating the spectral signal from the response of a transformation system. Bayesian (BIC) and Akaike (AIC) information criteria were assessed in order to provide the Gaussian mixture model (GMM) with the optimum number of clusters within the spectral space. The spectra of 2600 solar illuminations measured in Granada (Spain) were recovered over the range of 360–830 nm from their corresponding tristimulus values using a linear model of basis functions, the Wiener inverse (WI) method, and the Bayesian inverse approach extended to the GMM (BGMM). A model of Gaussian mixtures for solar irradiance was deemed to be more appropriate than a single Gaussian distribution for representing the probability distribution of the solar spectral data. The results showed that the estimation performance of the BGMM method was better than either the linear model or the WI method for the spectral approximation of daylight from the three-dimensional tristimulus values. © 2012 Optical Society of America

OCIS codes: 330.1690, 330.1730, 100.3190, 000.5490.

1. INTRODUCTION

Recent decades have witnessed a growing interest in the analysis of spectral signals applied to spectral compression and reconstruction. Thus, efficient spectral representation and color communication, together with the spectral analysis of solar illuminations and reflectance of colored samples, have been the subject of extensive research [1–7]. Within this context, the characteristics of the solar radiation spectrum in the ultraviolet, visible, and near-infrared regions is of crucial consideration in many disciplines, particularly in imaging, vision, and color science [8]. The spectral analysis of daylight irradiance under different atmospheric conditions has been an important subject in many applications of spectral daylight in imaging science where the color signal is studied, or in aspects of meteorology where solar spectral irradiance over a wide spectral range is investigated [9–13].

The vital need to be able to represent a large set of high-dimensional spectral data is fulfilled by a variety of models for spectral compression in a lower dimension of spectral space. The reverse stage, known as spectral recovery, involves decoding the compressed data in order to reconstruct the spectral data. Spectral daylight recovery and designing optimum sensors to estimate spectral irradiance, thus facilitating atmospheric research and applied meteorology, have been the focus of intense study in recent decades. In 1964, when Cohen [14] proposed a linear model depending on three components for surface spectral reflectances, Judd *et al.* [15] designed a three-dimensional linear model to fit the outdoor

spectral illumination. Following the development of linear models for spectral-reflectance reconstruction [1,16–18], many researchers turned their attention to the spectral recovery of illuminant spectra using linear models of basis functions extracted from the spectral-irradiance dataset. The spectral reconstruction of natural daylight in the visible range of the spectrum by a lower-dimensional linear combination of the eigenvectors obtained from the natural spectral dataset has been studied by Romero *et al.* and Hernández-Andrés *et al.* [19,20]. In 2004, Hernández-Andrés *et al.* [21] measured a set of 2600 daylight spectra in Granada (Spain) in order to study linear models for daylight spectral recovery using the responses of just a few sensors. They concluded that a suitable linear model can be accurately constructed with only five basis functions to recover outdoor daylight spectra within the visible range of 380–780 nm. A simple way of spectral approximation is based on a low-dimensional linear model of basis functions, which was that used in the research conducted by Slater and Healey [22] for daylight spectral reconstruction. These authors were of the opinion that global spectral-irradiance functions can be accurately fitted over the visible range by using a three-dimensional linear model, while an eight-dimensional linear model is required for accurate spectral recovery over the wider range of 400–2200 nm [22,23].

The problem of the performance of spectral recovery is more pressing when the responses of only a few sensors are available in practice for recovery over a broad spectral range, which is to say that the lower-dimensional sensor response

mathematically constrains the linear model from making use of more basis functions and thus the spectral range for accurate spectral reconstruction is constricted to a narrow range of the spectrum. Hence, the accurate recovery of a broader spectral range represented by more eigenvectors depends directly on the number of sensors, which should be equal to the number of basis functions in a linear spectral-recovery model. The Wiener inverse (WI) model as the probabilistic formulation of spectral recovery combines *a priori* information about the spectral data with the information obtained from measuring sensor signals. Thus, the model benefits from an *a priori* probability distribution of the training spectral dataset, which is often taken to follow a single Gaussian distribution. Regrettably, the spectral data can hardly follow a single Gaussian probability distribution. Taking only a single Gaussian density into account significantly compromises the accuracy of the estimation, and so a single Gaussian approximation is sometimes inadequate for characterizing the probability distribution of many real-world spectral datasets. Nevertheless, a mixture of Gaussian densities is a popular representation of non-Gaussian distributions. Thus, in order to improve the performance of the inverse model, a mixture of Gaussian distributions, known as the Gaussian mixture model (GMM), can be used as *a priori* information of the input spectral data.

In this paper, we describe a method of spectral recovery based on an extension of the Bayesian inverse approach to GMM. The method is used to approximate spectrally 2600 global spectral irradiances measured in Granada, Spain. The optimum number of Gaussian clusters of the training spectral-irradiance data is measured by evaluating the Bayesian (BIC) and Akaike (AIC) information criteria. The colorimetric and spectral performances of the proposed method are compared with the results obtained from a linear model and the WI approach for spectral reconstruction of spectral daylight.

2. THEORETICAL BACKGROUND

The linear transformation of the n -dimensional spectrum, \mathbf{r} , to the p -dimensional response, \mathbf{c} , can be formulated by

$$\mathbf{c} = \mathbf{A}^T \mathbf{r} + \boldsymbol{\epsilon}, \quad (1)$$

where \mathbf{A} is the $n \times p$ transformation matrix and $\boldsymbol{\epsilon}$ is the signal-independent additive noise of the system. The backward model of estimating spectrum \mathbf{r} from the response \mathbf{c} of the system in Eq. (1) is known as spectral reconstruction, which has recently been the subject of considerable investigation [24–31].

The basic backward model of estimating spectrum \mathbf{r} from the response vector \mathbf{c} can be created by a linear model of p basis functions, \mathbf{u}_j , extracted from the spectral dataset, $\mathcal{R}^n := \{\mathbf{r}_i\}_{i=1}^m$, in the following way:

$$\hat{\mathbf{r}} = \mathbf{S} \mathbf{c} + (\mathbf{I} - \mathbf{S} \mathbf{A}^T) \boldsymbol{\mu}_r, \quad (2)$$

where $\boldsymbol{\mu}_r$ is the mean vector of $\mathbf{r} \in \mathcal{R}^n$, and for a noiseless transformation system, $\mathbf{S} = \mathbf{U}(\mathbf{A}^T \mathbf{U})^{-1}$, in which the columns of the $n \times p$ matrix, \mathbf{U} , are the basis functions, \mathbf{u}_j [31].

Another way of spectral estimation is based on the Bayesian inference approach to the inverse problem of spectral recovery. The WI model, resulting from the Bayesian theorem, is widely used for spectral estimation and analysis in color and imaging applications [32–36]. Let us consider

the Bayes' theorem for estimating the posterior probability density function $p(\mathbf{r}|\mathbf{c})$, as follows:

$$p(\mathbf{r}|\mathbf{c}) = \frac{p(\mathbf{c}|\mathbf{r})p(\mathbf{r})}{p(\mathbf{c})}, \quad (3)$$

in which $p(\mathbf{c}|\mathbf{r})$ and $p(\mathbf{r})$ are the likelihood and prior probability density functions, respectively [37]. Assuming that prior probability, $p(\mathbf{r})$, follows a single Gaussian distribution, $\mathbf{r} \sim \mathcal{N}(\boldsymbol{\mu}_r, \boldsymbol{\Sigma}_r)$, as does noise, $\boldsymbol{\epsilon} \sim \mathcal{N}(\boldsymbol{\mu}_\epsilon, \boldsymbol{\Sigma}_\epsilon)$, then the posterior probability distribution, $p(\mathbf{r}|\mathbf{c}) = \mathcal{N}(\boldsymbol{\mu}_{r|\mathbf{c}}, \boldsymbol{\Sigma}_{r|\mathbf{c}})$, can be estimated, in which

$$\boldsymbol{\mu}_{r|\mathbf{c}} = \boldsymbol{\Xi}(\mathbf{c} - \boldsymbol{\mu}_\epsilon - \mathbf{A}^T \boldsymbol{\mu}_r) + \boldsymbol{\mu}_r, \quad (4)$$

$$\boldsymbol{\Sigma}_{r|\mathbf{c}} = \boldsymbol{\Sigma}_r - \boldsymbol{\Xi} \mathbf{A}^T \boldsymbol{\Sigma}_r, \quad (5)$$

and $\boldsymbol{\Xi} = \boldsymbol{\Sigma}_r \mathbf{A}(\mathbf{A}^T \boldsymbol{\Sigma}_r \mathbf{A} + \boldsymbol{\Sigma}_\epsilon)^{-1}$ is the Wiener estimation matrix. The mean vector and covariance matrix are represented by $\boldsymbol{\mu}$ and $\boldsymbol{\Sigma}$, respectively. The mean vector, $\boldsymbol{\mu}_{r|\mathbf{c}}$, of Eq. (4) can be taken as the most probable estimation of \mathbf{r} given response \mathbf{c} [37,38]. Both the linear model of Eq. (2) and the minimum-mean-square-error (MMSE) estimation of the WI approach, Eq. (4), are widely used in color science and imaging technology for spectral recovery and image restoration [2,24,39–42], yet the spectral performance of reconstruction methods based on the linear model and WI depends very much on the spectral characteristics of the primary dataset through the spectral range over which they were measured.

3. EXTENSION OF THE BAYESIAN INVERSE APPROACH TO THE GAUSSIAN MIXTURE MODEL

The probability distribution of prior information in the Bayesian inference model is important to the optimum performance of Bayesian-based methods. In practical applications of spectral signals or images, considering a single Gaussian model is rarely realistic [37]. In color applications the spectral analysis of reflecting specimens investigated by Attewell and Baddeley [43] provides sufficient evidence for the fact that reflectance spectra are better described by beta-distribution or a mixture of Gaussian distributions than a single normal distribution. Although many real-world stochastic systems exhibit non-Gaussian probability behavior, Gaussian mixture-density estimation can be adequately used to represent non-Gaussian systems. In 2002 Murakami *et al.* [44] proposed an appealing nonlinear approach for spectral recovery based on the GMM that could be considered for spectral reconstruction from the system response.

The GMM, as a very common representation of the density functions $p(\mathbf{r})$ for the stochastic vector, \mathbf{r} , can be represented by

$$p(\mathbf{r}) = \sum_{j=1}^L \omega_j \mathcal{N}(\mathbf{r}; \boldsymbol{\mu}_j, \boldsymbol{\Sigma}_j), \quad (6)$$

in which ω_j are nonnegative weighting coefficients with $\sum_j \omega_j = 1$ and $\mathcal{N}(\mathbf{r}; \boldsymbol{\mu}_j, \boldsymbol{\Sigma}_j)$ is the Gaussian density of the j th cluster with mean vector $\boldsymbol{\mu}_j$ and covariance matrix $\boldsymbol{\Sigma}_j$. Taking into account the prior distribution, $p(\mathbf{r})$, the posterior distribution, $p(\mathbf{r}|\mathbf{c})$, can be expressed by Eq. (7) (see Appendix A),

$$p(\mathbf{r}|\mathbf{c}) = \sum_{j=1}^L \omega_j^* \mathcal{N}(\mathbf{r}; \boldsymbol{\mu}_j^*, \boldsymbol{\Sigma}_j^*), \quad (7)$$

in which $\boldsymbol{\Sigma}_j^*$, $\boldsymbol{\mu}_j^*$, and ω_j^* are defined in Eqs. (A10), (A11), and (A15) respectively.

A. Estimation of the Recovered Signal

If the spectral signal \mathbf{r} follows a single Gaussian distribution, then $L = 1$, and the MMSE estimate of \mathbf{r} from the response vector \mathbf{c} is the mean vector, $\boldsymbol{\mu}_{r|\mathbf{c}}$, of Eq. (4), which minimizes $E\{\|\mathbf{r} - \hat{\mathbf{r}}\|^2\}$. Similarly, the following GMM-based estimation may be proposed for the recovered spectrum:

$$\hat{\mathbf{r}} = \sum_{j=1}^L \omega_j^* \boldsymbol{\mu}_j^*. \quad (8)$$

Maximum *a posteriori* (MAP) estimation of \mathbf{r} given response vector \mathbf{c} ,

$$\begin{aligned} \hat{\mathbf{r}}_{\text{MAP}} &= \underset{\mathbf{r}}{\operatorname{argmax}} \{p(\mathbf{r}|\mathbf{c})\} \\ &= \underset{\mathbf{r}}{\operatorname{argmax}} \left\{ \sum_{j=1}^L \omega_j^* \mathcal{N}(\mathbf{r}; \boldsymbol{\mu}_j^*, \boldsymbol{\Sigma}_j^*) \right\}, \end{aligned} \quad (9)$$

can be created by maximizing the posterior distribution of Eq. (7). Unfortunately, a closed-form analytical solution to Eq. (9) is not generally available. Nonetheless, the GMM-based MAP estimator of \mathbf{r} given \mathbf{c} for Eq. (7) can be approximately estimated by multivariate Taylor-series expansion of Gaussian component $p_j^*(\mathbf{r}) = \mathcal{N}(\mathbf{r}; \boldsymbol{\mu}_j^*, \boldsymbol{\Sigma}_j^*)$ as explained in Appendix B. Therefore the MAP estimator of \mathbf{r} given \mathbf{c} can be approximated by Eq. (10) using multivariate Taylor-series expansion of Gaussian probability density function $p_j^*(\mathbf{r})$ around vector $\tilde{\boldsymbol{\mu}}$,

$$\hat{\mathbf{r}}_{\text{MAP}} \approx - \left\{ \sum_{j=1}^L \omega_j^* \nabla^2 p_j^*(\tilde{\boldsymbol{\mu}}) \right\}^{-1} \sum_{j=1}^L \omega_j^* \{ \nabla p_j^*(\tilde{\boldsymbol{\mu}}) - \tilde{\boldsymbol{\mu}} \nabla^2 p_j^*(\tilde{\boldsymbol{\mu}}) \}. \quad (10)$$

In Eq. (10), $\tilde{\boldsymbol{\mu}}$ is a vector around which the MAP estimator $\hat{\mathbf{r}}_{\text{MAP}}$ is approximated. Thus we can take

$$\tilde{\boldsymbol{\mu}} = \underset{\mathbf{m} \in \mathcal{M}}{\operatorname{argmax}} \{p(\mathbf{m}|\mathbf{c})\}, \quad (11)$$

in which $\mathcal{M} = \{\boldsymbol{\mu}_1^*, \boldsymbol{\mu}_2^*, \dots, \boldsymbol{\mu}_L^*, \sum_{j=1}^L \omega_j^* \boldsymbol{\mu}_j^*\}$, as the closest vector to the actual MAP estimator $\hat{\mathbf{r}}_{\text{MAP}}$.

4. EXPERIMENTAL

A set of 2600 daylight spectra collected in Granada (Spain) [13] were used for spectral recovery. Figure 1 shows the CIE 1931 chromaticity coordinates of 2600 natural-daylight spectra overlaid with the CIE daylight and Planckian loci.

A. Clustering with Gaussian Mixtures

To fit a set of Gaussian mixtures to the training dataset as *a priori* information for the BGMM, the 2600 solar spectral irradiances must be classified to extract a given number of clusters from the training spectral data. The clusters can be assigned by classifying the training data using K -means clustering [45] and Gaussian mixture modeling [46,47]. In this research, the GMM was used to cluster the training dataset by

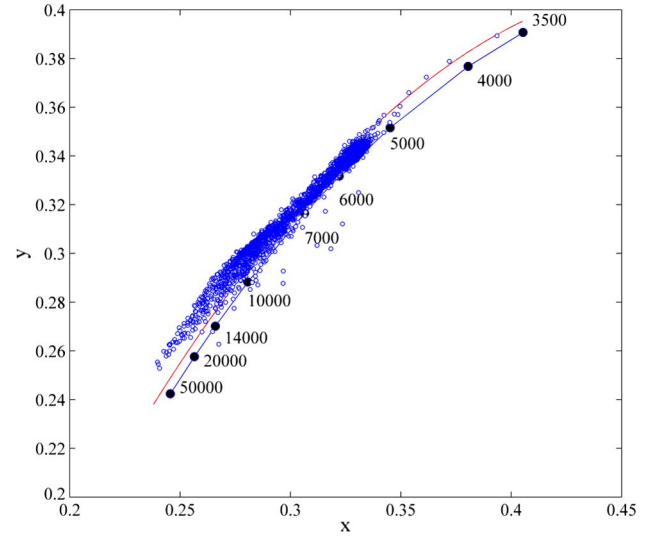


Fig. 1. (Color online) The CIE 1931 chromaticity coordinates of 2600 natural-daylight spectra (open blue circles) overlaid with the CIE daylight (red solid curve) and Planckian (blue solid curve with black circles) loci.

fitting the mixture models to the primary spectral data using the expectation maximization algorithm [48]. To find the optimum number of clusters for spectral illumination, BIC and AIC [49] were measured for the GMM with different numbers of clusters of the training spectral dataset. Equations (12) and (13) represent the AIC [50] and BIC [51] criteria, respectively:

$$\text{AIC} = -2 \ln \mathcal{L} + 2K, \quad (12)$$

$$\text{BIC} = -2 \ln \mathcal{L} + K \ln N, \quad (13)$$

in which \mathcal{L} is the likelihood function, K is the number of parameters of the model, and N is the number of data points. These calculations allow us to determine the appropriate number of Gaussian mixtures.

Figure 2 represents the AIC and BIC criteria for different numbers of clusters $L = 1, \dots, 8$. When the number of clusters increases from $L = 1$, corresponding to a single Gaussian model, to $L = 2$, related to two Gaussian mixtures, both the criteria decrease rapidly (Fig. 2). This confirms the superiority

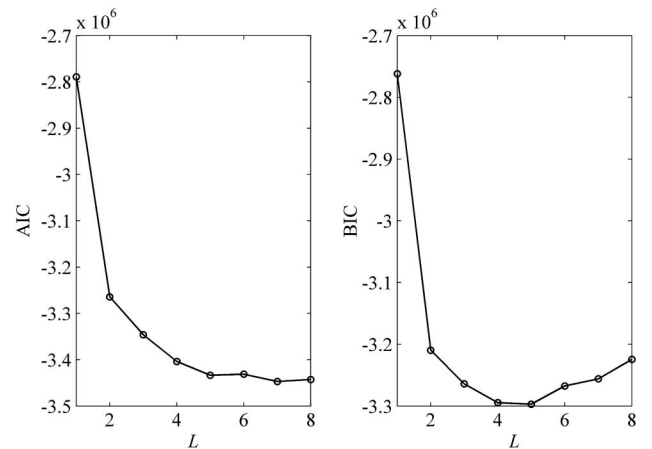


Fig. 2. BIC and AIC of GMM with different numbers of clusters $L = 1, \dots, 8$ created to represent the probability distribution of the primary spectral daylight illumination.

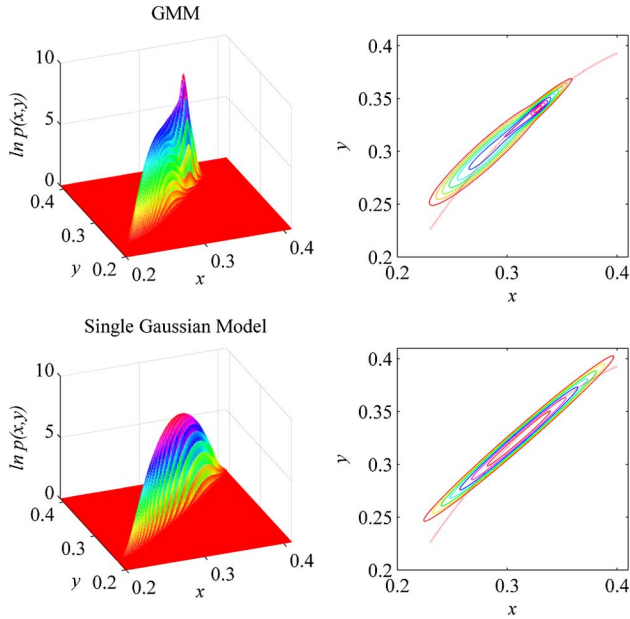


Fig. 3. (Color online) The log-*pdf* functions for the CIE 1931 chromaticity coordinates of 2600 natural-daylight spectra, the probability distributions of which were illustrated separately by the five Gaussian mixtures and a single Gaussian distribution. The contour lines for the two models are also shown in the figure.

of a GMM over the model represented by a single Gaussian distribution. It can be seen in Fig. 2 that the AIC criterion does not decrease significantly when the number of classes is more than five. Furthermore, the BIC criterion reaches its minimum value with a distribution of five Gaussian mixtures. Thus, a GMM with five optimum clusters ($L = 5$) was created to represent the probability distribution of the training spectral dataset.

Figure 3 shows the logarithm of probability density functions for the CIE 1931 chromaticity coordinates of the 2600 natural-daylight spectra that were represented by the

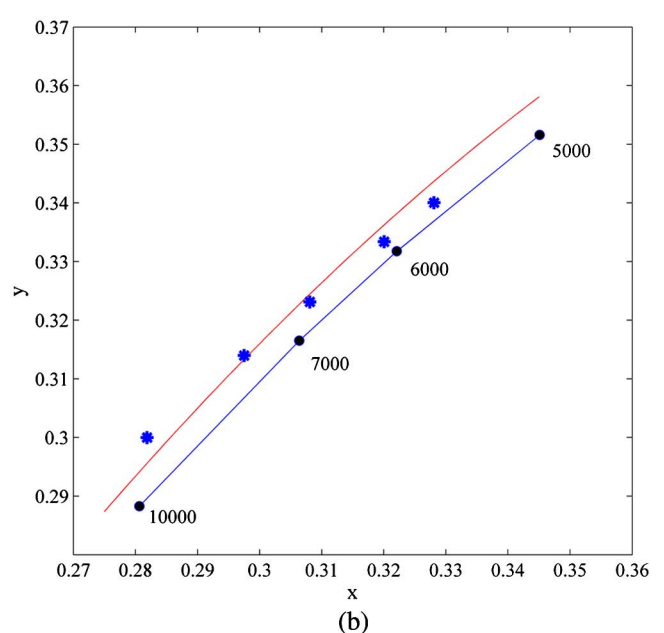
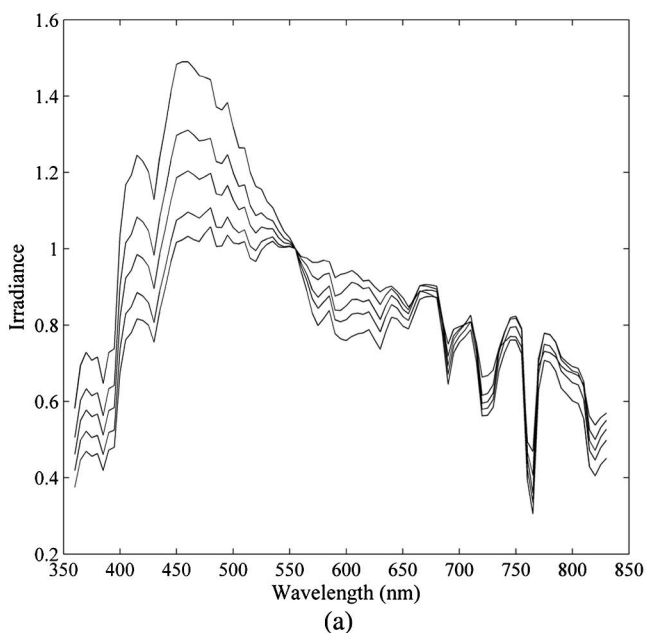


Fig. 4. (Color online) The spectra of the centers μ_j^* , $j = 1, \dots, 5$ of the five Gaussian clusters (a), and the corresponding chromaticity coordinates (b).

Table 1. Spectral and Colorimetric Performance of Spectral Reconstruction Using the Linear Model, the WI Approach, and the Bayesian Inverse Model Extended to the GMM (BGMM)^a

Method	% Feasible \hat{r}	Median	Mean
Linear	86.04	(0.9997, 0.1689)	(0.9985, 0.3220)
WI	85.69	(0.9998, 0.1688)	(0.9988, 0.2959)
BGMM	99.97	(0.9999, 0.1423)	(0.9990, 0.3069)

^aThe table shows the percentage of feasible recovered spectra together with the average and median of (GFC, ΔE_{uv}^*) measured between spectrum r and the feasible reconstructed \hat{r} for all the 2600 natural illuminations.

optimum five Gaussian mixtures and a single Gaussian distribution, respectively. The figure also shows the contour lines for the two models separately.

Figure 4(a) represents the relative spectral power distribution of the centers μ_j^* , $j = 1, \dots, 5$ of the five Gaussian clusters, together with their chromaticity coordinates. The correlated color temperatures (CCT) of the five centers were equal to 5633, 6015, 6700, 7455, and 9003 K. As can be seen from the chromaticity coordinates of the five centers of the clusters shown in Fig. 4(b), the varying CCT centers are sparsely distributed with different coordinates over the chromaticity diagram, resulting in an appropriate clustering of the training spectral data.

B. Spectral Reconstruction of Daylight Illumination

The 2600 outdoor daylight spectra were recovered using Eq. (8) from the corresponding CIE 1931 tristimulus values of the spectral illuminations. Spectral recovery was undertaken using three different methods: a linear approach from Eq. (2), the WI method described by Eq. (4), and an extension of the Bayesian inverse method to the GMM (BGMM) as expressed in Eq. (8). The spectral performances of the recovery approaches were assessed by the goodness-fitting coefficient (GFC)

$$GFC = \frac{\langle r, \hat{r} \rangle}{(r, r)^{1/2} (\hat{r}, \hat{r})^{1/2}}, \quad (14)$$

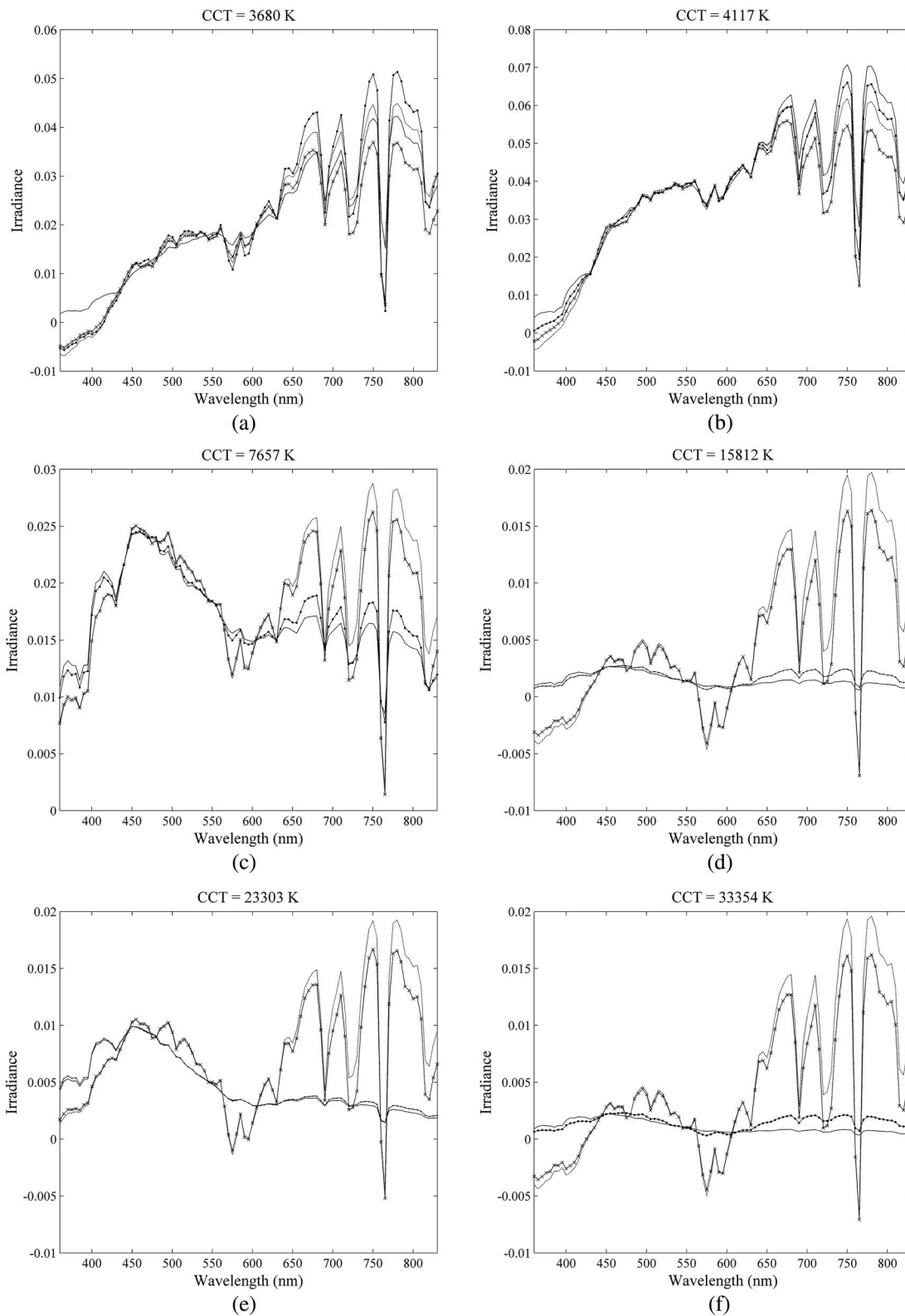


Fig. 5. Spectral recovery of the six natural outdoor illuminations (solid curve) using the linear model (dashed curve), the WI method (crossed curve), and the BGMM (dotted curve), presented for the spectral illuminations with CCT equal to (a) 3680, (b) 4117, (c) 7657, (d) 15812, (e) 23303, and (f) 33354 K.

where $\langle \cdot, \cdot \rangle$ is the operator for the inner product of the two vectors [20]. Furthermore, the colorimetric performance was measured by the CIELUV color difference formula, ΔE_{uv}^* , in which the coordinate of equal energy illuminant was taken as reference illumination.

The results of the spectral and colorimetric performances of the spectral reconstruction using the linear, WI, and BGMM models are set out in Table 1, in which the first value in the parentheses corresponds to the GFC and the second to ΔE_{uv}^* . Thus, the average and median of (GFC, ΔE_{uv}^*) measured

between spectrum r and the positive feasible reconstructed \hat{r} for all the 2600 natural illuminations are shown in Table 1. The table also shows separately the percentage of feasible positive recovered illumination spectra obtained from each recovery method. Comparing the results of spectral reconstruction obtained by the linear and WI approaches, it may be deduced that both performed similarly. Furthermore, the percentages of the feasible positive recovered spectra obtained by both approaches are close to 86. The results shown in this table reveal that the percentage of feasible recovered spectra obtained by the BGMM is 99.7, which is much higher than those achieved with the linear and WI approaches. The spectral and colorimetric performances of the BGMM spectral recovery method are also higher than those obtained with the linear and WI methods. Therefore, compared with the linear and WI methods, the BGMM can be regarded as a suitable approach to spectral recovery because it is not only more accurate in terms of spectral estimation but also provides a much higher percentage of feasible recovered spectra.

The six typical outdoor illuminations with CCTs of 3680, 4117, 7657, 15812, 23303, and 33354 K were spectrally recovered from the corresponding tristimulus values using the linear, WI, and BGMM approaches separately. The first spectrum, with CCT 3680 K, is located furthest away from the origin of the chromaticity diagram. The second selected spectrum is the second furthest point, with CCT equal to 4117 K. The coordinates of the selected spectra with increasing CCTs of 7657, 15812, and 23303 K approach the origin of the chromaticity diagram in such a way that the last selected spectrum, with CCT 33354 K, is the nearest coordinate to the origin, as can be seen in Fig. 5, in which the solid curve is spectrum r , while the dashed, crossed, and dotted curves represent the spectral illumination recovered by the linear, WI, and BGMM methods, respectively. It can be seen from Fig. 5(a) that none of the estimation methods resulted in a positive recovered spectrum, while in Fig. 5(b), only the BGMM yielded a positive estimated spectrum. Nevertheless, Fig. 5(c) shows that all the recovery approaches resulted in feasible positive reconstructed spectra, although the higher spectral performance of the BGMM is obvious in this figure. Nevertheless, feasible positive recovered spectra were not obtained in most cases of the illuminations recovered by the linear and WI methods. Interestingly, the BGMM resulted in positive recovered spectra in Figs. 5(b)–5(f). Furthermore, it can be seen in Fig. 5 that the spectral performance of the BGMM is appropriately higher than the linear and WI methods.

5. CONCLUSION

The extension of the Bayesian inverse approach to the GMM was proposed to recover the spectral signal more efficiently from the response of a transformation system. Thus, a numerical experiment was undertaken to perform the spectral reconstruction of 2600 natural-daylight spectra measured in Granada (Spain) using a linear approach, the WI method, and the Bayesian inverse approach extended to Gaussian mixtures. BIC and AIC measured for different numbers of clusters of the outdoor spectral illuminations showed that a model based on Gaussian mixtures represented the probability distribution of the training dataset

rather more closely than a single Gaussian distribution. The recovery performances of daylight spectral reconstruction of the linear and Wiener approaches were similar, resulting in about 86% feasible positive recovered spectra. The BGMM spectral-recovery method, on the other hand, resulted in 99.97% feasible positive recovered spectra, the spectral and colorimetric performances of which were convincingly more appropriate than those of the linear and WI models for spectral recovery. Finally, it should be pointed out that the technique described here of extending the Bayesian inverse approach to the GMM can be used for spectral signal estimation in many applications of imaging science and spectral signal processing.

APPENDIX A

Suppose that *a priori* the probability density function of spectrum r is given by the GMM

$$p(r) = \sum_{j=1}^L \omega_j ((2\pi)^n |\Sigma_j|)^{-1/2} \exp(\Gamma_j), \quad (\text{A1})$$

in which

$$\Gamma_j = -\frac{1}{2}(r - \mu_j)^T \Sigma_j^{-1} (r - \mu_j) \quad (\text{A2})$$

and ω_j are nonnegative weighting coefficients with $\sum_j \omega_j = 1$. Considering the noisy system of Eq. (1) with noise $\epsilon \sim \mathcal{N}(\mu_\epsilon, \Sigma_\epsilon)$, the likelihood function, $p(c|r)$, can be written as

$$p(c|r) = ((2\pi)^p |\Sigma_\epsilon|)^{-1/2} \exp(\Upsilon), \quad (\text{A3})$$

where

$$\Upsilon = -\frac{1}{2}[c - (\mathbf{A}^T r + \mu_\epsilon)]^T \Sigma_\epsilon^{-1} [c - (\mathbf{A}^T r + \mu_\epsilon)]. \quad (\text{A4})$$

Given the noisy system of Eq. (1) and the probability density functions $p(r)$ for the spectrum r , and $p(\epsilon)$ for noise ϵ , the probability density function $p(c)$ can be created by the following:

$$p(c) = \sum_{j=1}^L \omega_j ((2\pi)^p |\mathbf{K}_j|)^{-1/2} \exp(\Phi_j), \quad (\text{A5})$$

in which $\mathbf{K}_j = \mathbf{A}^T \Sigma_j \mathbf{A} + \Sigma_\epsilon$ and

$$\Phi_j = -\frac{1}{2}(c - \kappa_j)^T \mathbf{K}_j^{-1} (c - \kappa_j), \quad (\text{A6})$$

where $\kappa_j = \mathbf{A}^T \mu_j + \mu_\epsilon$. By incorporating $p(r)$, $p(c|r)$, and $p(\epsilon)$ from Eqs. (A1), (A3), and (A5), respectively, into Eq. (3), we get the following:

$$\begin{aligned}
p(\mathbf{r}|\mathbf{c}) &= \frac{((2\pi)^p |\Sigma_\epsilon|)^{-1/2} \exp(\Upsilon) \sum_{j=1}^L \omega_j ((2\pi)^n |\Sigma_j|)^{-1/2} \exp(\Gamma_j)}{\sum_{j=1}^L \omega_j ((2\pi)^p |\mathbf{K}_j|)^{-1/2} \exp(\Phi_j)} \\
&= \frac{((2\pi)^p |\Sigma_\epsilon|)^{-1/2} \sum_{j=1}^L \omega_j ((2\pi)^n |\Sigma_j|)^{-1/2} \exp(\Phi_j) \exp(\Upsilon + \Gamma_j - \Phi_j)}{\sum_{j=1}^L \omega_j ((2\pi)^p |\mathbf{K}_j|)^{-1/2} \exp(\Phi_j)}. \tag{A7}
\end{aligned}$$

In Eq. (A7), $\Gamma_j^* = \Upsilon + \Gamma_j - \Phi_j$ can be written by taking into account Eqs (A2), (A4), and (A6) as follows:

$$\begin{aligned}
\Gamma_j^* &= -\frac{1}{2} [\mathbf{c} - (\mathbf{A}^T \mathbf{r} + \boldsymbol{\mu}_\epsilon)]^T \Sigma_\epsilon^{-1} [\mathbf{c} - (\mathbf{A}^T \mathbf{r} + \boldsymbol{\mu}_\epsilon)] \\
&\quad - \frac{1}{2} (\mathbf{r} - \boldsymbol{\mu}_j)^T \Sigma_j^{-1} (\mathbf{r} - \boldsymbol{\mu}_j) + \frac{1}{2} (\mathbf{c} - \boldsymbol{\kappa}_j)^T \mathbf{K}_j^{-1} (\mathbf{c} - \boldsymbol{\kappa}_j), \tag{A8}
\end{aligned}$$

which can be rewritten as

$$\Gamma_j^* = -\frac{1}{2} (\mathbf{r} - \boldsymbol{\mu}_j^*)^T \Sigma_j^{*-1} (\mathbf{r} - \boldsymbol{\mu}_j^*), \tag{A9}$$

where

$$\Sigma_j^* = (\Sigma_j^{-1} + \mathbf{A} \Sigma_\epsilon^{-1} \mathbf{A}^T)^{-1}, \tag{A10}$$

$$\boldsymbol{\mu}_j^* = \Sigma_j^* (\Sigma_j^{-1} \boldsymbol{\mu}_j + \mathbf{A} \Sigma_\epsilon^{-1} \mathbf{c} - \mathbf{A} \Sigma_\epsilon^{-1} \boldsymbol{\mu}_\epsilon). \tag{A11}$$

Using a generalized form of Sylvester's determinant theorem [52], it can be shown that

$$\begin{aligned}
\frac{((2\pi)^p |\Sigma_\epsilon|)^{-1/2} ((2\pi)^n |\Sigma_j|)^{-1/2}}{((2\pi)^p |\mathbf{K}_j|)^{-1/2}} &= ((2\pi)^n |\Sigma_j^{-1} + \mathbf{A} \Sigma_\epsilon^{-1} \mathbf{A}^T|)^{-1/2} \\
&= ((2\pi)^n |\Sigma_j^*|)^{-1/2}. \tag{A12}
\end{aligned}$$

Equation (A7) can be rewritten using Eq. (A12) as

$$p(\mathbf{r}|\mathbf{c}) = \frac{\sum_{j=1}^L \omega_j ((2\pi)^p |\mathbf{K}_j|)^{-1/2} ((2\pi)^n |\Sigma_j^*|)^{-1/2} \exp(\Phi_j) \exp(\Gamma_j^*)}{\sum_{j=1}^L \omega_j ((2\pi)^p |\mathbf{K}_j|)^{-1/2} \exp(\Phi_j)}, \tag{A13}$$

to create the following form of GMM for the posterior distribution $p(\mathbf{r}|\mathbf{c})$:

$$p(\mathbf{r}|\mathbf{c}) = \sum_{j=1}^L \omega_j^* ((2\pi)^n |\Sigma_j^*|)^{-1/2} \exp(\Gamma_j^*), \tag{A14}$$

in which ω_j^* are the nonnegative weights

$$\begin{aligned}
\omega_j^* &= \frac{\omega_j ((2\pi)^p |\mathbf{K}_j|)^{-1/2} \exp(\Phi_j)}{\sum_{j=1}^L \omega_j ((2\pi)^p |\mathbf{K}_j|)^{-1/2} \exp(\Phi_j)} \\
&= \frac{\omega_j \mathcal{N}(\mathbf{c}; \boldsymbol{\kappa}_j, \mathbf{K}_j)}{\sum_{j=1}^L \omega_j \mathcal{N}(\mathbf{c}; \boldsymbol{\kappa}_j, \mathbf{K}_j)} \tag{A15}
\end{aligned}$$

with $\sum_j \omega_j^* = 1$.

Furthermore, using the Sherman–Morison–Woodbury formula in matrix algebra [53], Eqs. (A10) and (A11) can be

rewritten respectively as follows (see also Eqs. (145)–(147) in [54]):

$$\Sigma_j^* = \Sigma_j - \mathbf{S}_j \mathbf{A}^T \Sigma_j, \tag{A16}$$

$$\boldsymbol{\mu}_j^* = \mathbf{S}_j (\mathbf{c} - \boldsymbol{\mu}_\epsilon - \mathbf{A}^T \boldsymbol{\mu}_j) + \boldsymbol{\mu}_j, \tag{A17}$$

in which

$$\mathbf{S}_j = \Sigma_j \mathbf{A} (\mathbf{A}^T \Sigma_j \mathbf{A} + \Sigma_\epsilon)^{-1} = \Sigma_j \mathbf{A} \mathbf{K}_j^{-1}. \tag{A18}$$

APPENDIX B

Multivariate Taylor-series expansion of the Gaussian probability distribution $p(\mathbf{x})$ around vector $\tilde{\boldsymbol{\mu}}$ can be written as

$$p(\mathbf{x}) = \sum_{k=0}^R \frac{1}{k!} ((\mathbf{x} - \tilde{\boldsymbol{\mu}}) \odot \nabla)^k p(\mathbf{x})|_{\mathbf{x}=\tilde{\boldsymbol{\mu}}} + O_R, \tag{B1}$$

in which ∇ is the gradient with respect to \mathbf{x} , O_R is the remainder term, and \odot is the matrix operator for two matrices with the same dimensions, which is an elementwise matrix multiplication and a subsequent summation of all matrix elements [55]. Considering Eq. (B1), multivariate Taylor-series expansion of the j th Gaussian distribution $p_j^*(\mathbf{r}) = \mathcal{N}(\mathbf{r}; \boldsymbol{\mu}_j^*, \Sigma_j^*)$ around vector $\tilde{\boldsymbol{\mu}}$ can be approximated by

$$\begin{aligned}
p_j^*(\mathbf{r}) &= p_j^*(\tilde{\boldsymbol{\mu}}) + (\mathbf{r} - \tilde{\boldsymbol{\mu}})^T \nabla p_j^*(\tilde{\boldsymbol{\mu}}) + \frac{1}{2!} (\mathbf{r} - \tilde{\boldsymbol{\mu}})^T \nabla^2 p_j^*(\tilde{\boldsymbol{\mu}}) (\mathbf{r} - \tilde{\boldsymbol{\mu}}) \\
&\quad + \frac{1}{3!} \{[(\mathbf{r} - \tilde{\boldsymbol{\mu}})(\mathbf{r} - \tilde{\boldsymbol{\mu}})^T] \otimes (\mathbf{r} - \tilde{\boldsymbol{\mu}})\} \odot \nabla^3 p_j^*(\tilde{\boldsymbol{\mu}}) + \dots, \tag{B2}
\end{aligned}$$

in which \otimes is the Kronecker product operator. In Eq. (B2), the first-order derivative is

$$\nabla p_j^*(\mathbf{x}) = -\Sigma_j^{*-1} (\mathbf{x} - \boldsymbol{\mu}_j^*) p_j^*(\mathbf{x}), \tag{B3}$$

the second-order derivative or Hessian matrix $\mathbf{H}(\mathbf{x})$ is

$$\nabla^2 p_j^*(\mathbf{x}) = \mathbf{H}_j(\mathbf{x}) = -\Sigma_j^{*-1} [(\mathbf{x} - \boldsymbol{\mu}_j^*) (\nabla p_j^*(\mathbf{x}))^T + p_j^*(\mathbf{x})], \tag{B4}$$

and third-order derivative is given by

$$\begin{aligned}
\nabla^3 p_j^*(\mathbf{x}) &= -\mathbf{H}_j(\mathbf{x}) \otimes (\Sigma_j^{*-1} (\mathbf{x} - \boldsymbol{\mu}_j^*)) - \nabla p_j^*(\mathbf{x}) \\
&\quad \otimes \Sigma_j^{*-1} - \text{vec}(\Sigma_j^{*-1}) (\nabla p_j^*(\mathbf{x}))^T, \tag{B5}
\end{aligned}$$

where $\text{vec}(\cdot)$ denotes an operator that vectorizes a matrix by stacking its columns [54–56]. Thus, the second-order

multivariate Taylor-series approximation of Eq. (A14) around vector $\tilde{\boldsymbol{\mu}}$ is

$$p(\mathbf{r}|\mathbf{c}) \approx \sum_{j=1}^L \omega_j^* \left\{ p_j^*(\tilde{\boldsymbol{\mu}}) + (\mathbf{r} - \tilde{\boldsymbol{\mu}})^T \nabla p_j^*(\tilde{\boldsymbol{\mu}}) + \frac{1}{2} (\mathbf{r} - \tilde{\boldsymbol{\mu}})^T \nabla^2 p_j^*(\tilde{\boldsymbol{\mu}}) (\mathbf{r} - \tilde{\boldsymbol{\mu}}) \right\}. \quad (\text{B6})$$

The MAP estimate of \mathbf{r} given \mathbf{c} is obtained by maximizing $p(\mathbf{r}|\mathbf{c})$, which can be achieved by setting the derivative of $p(\mathbf{r}|\mathbf{c})$ with respect to \mathbf{r} equal to zero:

$$\frac{\partial p(\mathbf{r}|\mathbf{c})}{\partial \mathbf{r}} = 0. \quad (\text{B7})$$

By incorporating the approximate Eq. (B6) for $p(\mathbf{r}|\mathbf{c})$ and Eq. (B7), and considering the principles of differentiation of matrix functions [54,56], we can write

$$\frac{\partial p(\mathbf{r}|\mathbf{c})}{\partial \mathbf{r}} \approx \sum_{j=1}^L \omega_j^* \{ \nabla p_j^*(\tilde{\boldsymbol{\mu}}) + \mathbf{H}_j(\tilde{\boldsymbol{\mu}}) (\mathbf{r} - \tilde{\boldsymbol{\mu}}) \} = 0. \quad (\text{B8})$$

Solving Eq. (B8) for \mathbf{r} , we obtain

$$\hat{\mathbf{r}}_{\text{MAP}} \approx - \left\{ \sum_{j=1}^L \omega_j^* \mathbf{H}_j(\tilde{\boldsymbol{\mu}}) \right\}^{-1} \sum_{j=1}^L \omega_j^* \{ \nabla p_j^*(\tilde{\boldsymbol{\mu}}) - \tilde{\boldsymbol{\mu}} \mathbf{H}_j(\tilde{\boldsymbol{\mu}}) \}, \quad (\text{B9})$$

which is approximately the MAP estimator of \mathbf{r} given \mathbf{c} .

ACKNOWLEDGMENT

The facilities and scientific and technical assistance provided by the Department of Optics at the University of Granada in Spain are greatly acknowledged and appreciated.

REFERENCES

- J. Parkkinen, J. Hallikainen, and T. Jääskeläinen, "Characteristic spectra of Munsell colors," *J. Opt. Soc. Am. A* **6**, 318–322 (1989).
- A. Garcia-Beltrán, J. L. Nieves, J. Hernández-Andrés, and J. Romero, "Linear bases for spectral reflectance functions of acrylic paints," *Color Res. Appl.* **23**, 39–45 (1998).
- G. Healey and L. Benites, "Linear models for spectral reflectance functions over the mid-wave and long-wave infrared," *J. Opt. Soc. Am. A* **15**, 2216–2227 (1998).
- C. Chiao, D. Osorio, M. Vorobyev, and T. W. Cronin, "Characterization of natural illuminants in forests and the use of digital video data to reconstruct illuminant spectra," *J. Opt. Soc. Am. A* **17**, 1713–1721 (2000).
- A. K. Romney and T. Indow, "A model for the simultaneous analysis of reflectance spectra and basis factors of Munsell color samples under D65 illumination in three-dimensional euclidean space," *Proc. Natl. Acad. Sci. USA* **99**, 11543–11546 (2002).
- O. Kohonen, J. Parkkinen, and T. Jääskeläinen, "Databases for spectral color science," *Color Res. Appl.* **31**, 381–390 (2006).
- T. Indow and A. K. Romney, "Reflectance spectra of Munsell standard chips and their appearance," *Color Res. Appl.* **33**, 229–237 (2008).
- G. Wyszecki and W. S. Stiles, *Color Science: Concepts and Methods, Quantitative Data and Formula* (Wiley, 1982).
- S. R. Das and V. D. P. Sastri, "Spectral distribution and color of tropical daylight," *J. Opt. Soc. Am.* **55**, 319–322 (1965).
- S. R. Das and V. D. P. Sastri, "Spectral distribution and color of north sky at Delhi," *J. Opt. Soc. Am.* **56**, 829–830 (1966).
- S. R. Das and V. D. P. Sastri, "Typical spectral distributions and color for tropical daylight," *J. Opt. Soc. Am.* **58**, 391–398 (1968).
- E. Dixon, "Spectral distribution of Australian daylight," *J. Opt. Soc. Am.* **68**, 437–450 (1978).
- J. Hernández-Andrés, J. Romero, J. L. Nieves, and R. L. Lee, Jr., "Color and spectral analysis of daylight in southern Europe," *J. Opt. Soc. Am. A* **18**, 1325–1335 (2001).
- J. B. Cohen, "Dependency of the spectral reflectance curves of the Munsell color chips," *Psychonomic Sci.* **1**, 369–370 (1994).
- D. B. Judd, D. L. MacAdam, G. Wyszecki, H. W. Budde, H. R. Condit, S. T. Henderson, and J. L. Simonds, "Spectral distribution of typical daylight as a function of correlated color temperature," *J. Opt. Soc. Am.* **54**, 1031–1040 (1964).
- L. T. Maloney and B. A. Wandell, "Color constancy: a method for recovering surface spectral reflectance," *J. Opt. Soc. Am. A* **3**, 29–33 (1986).
- L. T. Maloney, "Evaluation of linear models of surface spectral reflectance with small numbers of parameters," *J. Opt. Soc. Am. A* **3**, 1673–1683 (1986).
- D. H. Marimont and B. A. Wandell, "Linear models of surface and illuminant spectra," *J. Opt. Soc. Am. A* **9**, 1905–1913 (1992).
- J. Romero, A. Garcia-Beltrán, and J. Hernández-Andrés, "Linear bases for representation of natural and artificial illuminants," *J. Opt. Soc. Am. A* **14**, 1007–1014 (1997).
- J. Hernández-Andrés, J. Romero, A. Garcia-Beltrán, and J. L. Nieves, "Testing linear models on spectral daylight measurements," *Appl. Opt.* **37**, 971–977 (1998).
- J. Hernández-Andrés, J. L. Nieves, E. M. Valero, and J. Romero, "Spectral-daylight recovery by use of only a few sensors," *J. Opt. Soc. Am. A* **21**, 13–23 (2004).
- D. Slater and G. Healey, "Analyzing the spectral dimensionality of outdoor visible and near-infrared illumination functions," *J. Opt. Soc. Am. A* **15**, 2913–2920 (1998).
- Z. Pan, G. Healey, and D. Slater, "Global spectral irradiance variability and material discrimination at Boulder, Colorado," *J. Opt. Soc. Am. A* **20**, 513–521 (2003).
- D. H. Brainard, "Bayesian method for reconstructing color images from trichromatic samples," in *Proceedings of the IS&T 47th Annual Conference* (IS&T, 1995), pp. 375–380.
- H. S. Fairman and M. H. Brill, "The principal components of reflectances," *Color Res. Appl.* **29**, 104–110 (2004).
- F. M. Abed, S. H. Amirshahi, S. Peyvandi, and M. R. M. Abed, "Reconstruction of the reflectance curves by using interpolation method," in *Proceedings of AIC 2007—Color Science for Industry*, midterm meeting of the International Color Association (2007).
- F. Agahian, S. A. Amirshahi, and S. H. Amirshahi, "Reconstruction of reflectance spectra using weighted principal component analysis," *Color Res. Appl.* **33**, 360–371 (2008).
- T. Harfi, S. H. Amirshahi, and F. Agahian, "Recovery of reflectance spectra from colorimetric data using principal component analysis embedded regression technique," *Opt. Rev.* **15**, 302–308 (2008).
- T. Eslahi, S. H. Amirshahi, and F. Agahian, "Recovery of spectral data using weighted canonical correlation regression," *Opt. Rev.* **16**, 296–303 (2009).
- S. A. Amirshahi and S. H. Amirshahi, "Adaptive non-negative bases for reconstruction of spectral data from colorimetric information," *Opt. Rev.* **17**, 562–569 (2010).
- S. Peyvandi and S. H. Amirshahi, "Generalized spectral decomposition: a theory and practice to spectral reconstruction," *J. Opt. Soc. Am. A* **28**, 1545–1553 (2011).
- Y. Murakami, K. Fukura, M. Yamaguchi, and N. Ohyama, "Color reproduction from low-snr multispectral images using spatio-spectral wiener estimation," *Opt. Express* **16**, 4106–4120 (2008).
- N. Shimano, "Recovery of spectral reflectances of objects being imaged without prior knowledge," *IEEE Trans. Image Process.* **15**, 1848–1856 (2006).
- N. Shimano, K. Terai, and M. Hironaga, "Recovery of spectral reflectances of objects being imaged by multispectral cameras," *J. Opt. Soc. Am. A* **24**, 3211–3219 (2007).
- N. Shimano, "Optimization of spectral sensitivities with gaussian distribution functions for a color image acquisition device in the presence of noise," *Opt. Eng.* **45**, 013201 (2006).

36. N. Shimano and M. Hironaga, "Recovery of spectral reflectances of imaged objects by the use of features of spectral reflectances," *J. Opt. Soc. Am. A* **27**, 251–258 (2010).
37. A. Mohammad-Djafari, "Bayesian inference for inverse problems in signal and image processing and applications," *Int. J. Imaging Syst. Tech.* **16**, 209–214 (2006).
38. M. Bertero and P. Boccacci, *Introduction to Inverse Problems in Imaging* (Institute of Physics, 1998).
39. D. Tzeng and R. S. Berns, "A review of principal component analysis and its applications to color technology," *Color Res. Appl.* **30**, 84–98 (2005).
40. D. H. Brainard and W. T. Freeman, "Bayesian color constancy," *J. Opt. Soc. Am. A* **14**, 1393–1411 (1997).
41. V. Heikkinen, R. Lenz, T. Jetsu, J. Parkkinen, M. Hauta-Kasari, and T. Jääskeläinen, "Evaluation and unification of some methods for estimating reflectance spectra from RGB images," *J. Opt. Soc. Am. A* **25**, 2444–2458 (2008).
42. Y. Murakami, K. Ietom, M. Yamaguchi, and N. Ohyama, "Maximum a posteriori estimation of spectral reflectance from color image and multipoint spectral measurements," *Appl. Opt.* **46**, 7068–7082 (2007).
43. D. Attewell and R. J. Baddeley, "The distribution of reflectances within the visual environment," *Vis. Res.* **47**, 548–554 (2007).
44. Y. Murakami, T. Obi, M. Yamaguchi, and N. Ohyama, "Nonlinear estimation of spectral reflectance based on gaussian mixture distribution for color image reproduction," *Appl. Opt.* **41**, 4840–4847 (2002).
45. J. MacQueen, "Some methods for classification and analysis of multivariate observations," in *Proceedings of the 5th Berkeley Symposium on Mathematical Statistics and Probability* (University of California, 1967), pp. 281–297.
46. A. Dempster, N. Laird, and D. Rubin, "Maximum likelihood from incomplete data via the EM algorithm," *J. R. Stat. Soc. Ser. B. Methodol.* **39B**, 1–38 (1977).
47. M. A. T. Figueiredo and A. K. Jain, "Unsupervised learning of finite mixture models," *IEEE Trans. Pattern Anal. Machine Intell.* **24**, 381–396 (2002).
48. G. McLachlan and D. Peel, *Finite Mixture Models* (Wiley, 2000).
49. A. R. Liddle, "Information criteria for astrophysical model selection," *Mon. Not. R. Astron. Soc.* **377**, L74–L78 (2007).
50. H. Akaike, "A new look at the statistical model identification," *IEEE Trans. Autom. Control* **19**, 716–723 (1974).
51. G. Schwarz, "Estimating the dimension of a model," *Ann. Stat.* **6**, 461–464 (1978).
52. D. A. Harville, *Matrix Algebra From A Statistician's Perspective* (Springer, 2008), pp. 419–420.
53. A. J. Laub, *Matrix Analysis for Scientists & Engineers* (SIAM, 2005), p. 48.
54. K. B. Petersen and M. S. Pedersen, "The matrix cookbook," <http://matrixcookbook.com> (14 Nov. 2008).
55. M. F. Huber, T. Bailey, H. Durrant-Whyte, and U. D. Hanebeck, "On entropy approximation for gaussian mixture random vectors," in *IEEE International Conference on Multisensor Fusion and Integration for Intelligent Systems* (IEEE, 2008), pp. 181–188.
56. P. S. Dwyer, "Some applications of matrix derivatives in multivariate analysis," *J. Am. Stat. Assoc.* **62**, 607–625 (1967).